Ab Initio Modeling of Amide Vibrational Bands in Solution

Nicholas A. Besley*

School of Chemistry, University of Nottingham, University Park, Nottingham NG7 2RD, United Kingdom

Received: August 31, 2004; In Final Form: September 29, 2004

A combination of molecular dynamics simulations and density functional theory has been used to model the band profiles of the amide I, II, and III vibrational modes of *trans-N*-methylacetamide in water and acetonitrile. From these calculations, the band shapes can be predicted. Solvent affects the different amide modes differently. The dependence of the solvatochromic shifts in frequency and intensity on the position of the solvent molecules has been studied. These shifts are described by empirical fits of data generated through density functional theory calculations of model systems. Band profiles are simulated on the basis of 8000 structures drawn from molecular dynamics simulations. Frequencies are predicted with an error of less than 13 cm^{-1}. The full width at half-maximum of the predicted bands are also in good agreement with experiment and indicate that hydrogen bonding plays an important role in the broadening of the spectral bands.

Introduction

Infrared (IR) spectroscopy provides a probe of polypeptide and protein secondary structure.[1] The amide I, II, and III bands are the most useful in structure designation and correspond to vibrational modes associated with the amide group. The amide I band is the most intense and is predominantly C═O stretch. The amide II and amide III bands arise from the out-of-phase and in-phase combinations of the NH in plane bend and CN stretch, respectively. Currently, there is an ongoing effort to study these amide bands.[2−16] Recently, two-dimensional time-resolved spectroscopic techniques have been applied to study peptides.[4,5,7,11] The focus of much of this work has been small amides, such as *trans-N*-methylacetamide (NMA), since these serve as simple models of the peptide linkage.

The IR spectroscopy of amides has also been the subject of extensive theoretical investigations; much of this work is summarized elsewhere.[17] Calculation of anharmonic vibrational frequencies for molecules such as NMA is too demanding computationally, and harmonic frequencies are usually computed. In the gas phase, harmonic frequencies computed using density functional theory (DFT) with the EDF1 exchange-correlation functional[18] and the 6-31+G* basis set reproduce experiment accurately.[17] The majority of theoretical studies model an isolated molecule. However, most experiments are performed in solution. Solvent has a dramatic effect on the amide modes.[9] For NMA in water, the amide I mode is red-shifted by ∼100 cm^{-1} and the amide II and III modes are blue-shifted by ∼80 cm^{-1} and ∼60 cm^{-1}, respectively.[9] In addition, the amide I band becomes more intense relative to the amide II and III bands. In less polar solvents, the solvatochromic shifts are smaller but remain significant.[9] In acetonitrile, a red-shift of ∼60 cm^{-1} for the amide I band and blue-shifts of ∼50 cm^{-1} and ∼30 cm^{-1} for the amide II and III bands are observed.[9] These shifts can be understood qualitatively by considering the resonance structures of NMA (Figure 1). Polar solvents will stabilize the ionic form, leading to a weakening of the C═O bond and a strengthening of the CN bond. This would result in a red-shift in the amide I mode and blue-shift in the amide II and III modes. The greater polarization would lead to increase in band intensities, particularly for the amide I mode. It is precisely this sensitivity of the amide bands to their local environment that enables them to act as a measure of secondary structure. Currently, protein amide bands are computed using the transition dipole coupling method.[19,20] This method captures the electrostatic interaction between oscillating dipoles representing the C═O vibration. It has been suggested that changes in the diagonal terms of the force constant matrix because of hydrogen bonding could be significant.[3,15] Clearly, the development of theoretical models that capture the influence of the local environment on the amide bands is important. A significant step toward this goal is the calculation of the amide bands in solution.

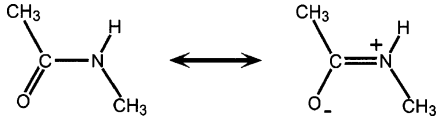

Figure 1. Resonance structures of *N*-methylacetamide.

The inclusion of solvent within ab initio calculations of IR spectra is problematic, and several approximate treatments are widely used. In the simplest model, the solute lies in a cavity embedded in solvent described by a continuum dielectric.[21] Such implicit solvent models do not account for hydrogen bonding and have been shown to underestimate the solvatochromic shifts for NMA.[3,9] Alternatively, explicit solvent molecules can be included within the ab initio treatment. However, the rapid rise in computational cost means it is not possible to include sufficient molecules to provide an adequate description of bulk solvent. Combining these approaches by including a small number of explicit water molecules within the cavity does give good agreement with experiment.[3,9] Typically, three water molecules in the three hydrogen bonding sites of NMA (see Figure 2) are included.[22]

Torii et al.[3] studied the amide bands in the NMA-3H_2O cluster at the Hartree−Fock/6-31++G** level with a self-consistent reaction field. In this study, three water molecules in conjunction with the reaction field captured the effect of solvent on the NMA vibrational force field. A correlation between the C═O bond length and frequency of the amide I mode was also observed.

* E-mail: nick.besley@nottingham.ac.uk; fax: +44 115 951 3562.

10.1021/jp046073c CCC: $27.50
Published on Web 11/12/2004

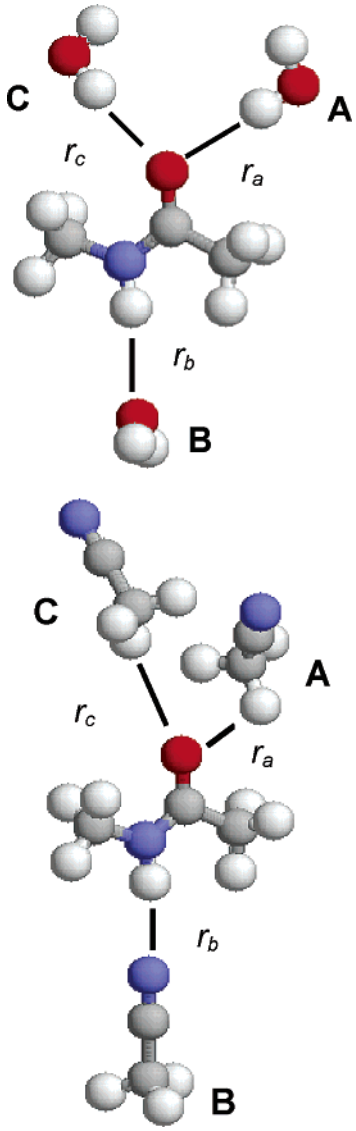

Figure 2. Structures of NMA-3H_2O and NMA-3MeCN clusters.

Furthermore, changes in Raman intensities of the amide bands were consistent with structural changes. Kubelka and Keiderling[9] reported experimental IR spectra for NMA in water and acetonitrile. DFT calculations with modified basis sets were used to model the IR frequencies in water with a range of explicit and continuum solvent models. These calculations also showed that a combination of three water molecules embedded in a continuum dielectric provides good agreement with experiment.

Calculations of this type provide a single snapshot of NMA in solution. A further level of complexity is to account for the many configurations that the solvent molecules can adopt. Such calculations can describe the broadening of the spectral bands induced by the environment. This is particularly relevant for the amide bands since both their location and shape provide secondary structure information.[23] The most rigorous approach to this problem would be through Car−Parrinello molecular dynamics simulations.[24,25] However, the interest in studying large polypeptides has led researchers to pursue computationally less demanding techniques. Solvent configurations can be generated readily through classical molecular dynamics (MD) simulations. However, if many thousand configurations are to be sampled or large systems studied, much cheaper methods of evaluating the vibrational frequencies and intensities must be used.

Cho and co-workers[12,13,26] developed an empirical correction for the amide I mode of NMA in water. Their model exploited the relationship between the changes in the C═O bond length and the electrostatic potential at the atomic sites of NMA arising from the charge distribution of the surrounding water molecules. Since a linear correlation between the C═O bond length and amide I frequency has been observed,[3,12] the solvated band frequency can be evaluated. A small number of parameters were fitted using Hartree−Fock/6-311++G** calculations of NMA-$n$$D_2O$ (n = 5) clusters.[12] The amide I band of NMA in water was calculated on the basis of structures from a MD simulation.[13] The ensemble average frequency shift was −78 cm^{-1}. The computed band profile had a full width at half-maximum (fwhm) of 38 cm^{-1}, which reduced to 26.9 cm^{-1} when accounting for lifetime broadening. This was in good agreement with the value of 29 cm^{-1} from experiment.[7] This empirical correction was later reparametrized on the basis of DFT calculations of clusters extracted from an MD simulation.[14] A frequency shift of −80 cm^{-1} was evaluated for the NMA amide I band and a solvent corrected spectrum for a pentapeptide was reported. However, extension of this approach to arbitrary vibrational modes is problematic. In particular, nonlocal modes, such as amide II, could not be modeled successfully.[14] The amide I mode of NMA in methanol has also been studied. The computed band profile is asymmetric and could be decomposed into two Gaussian bands associated with two distinct solvation structures.[27]

In this paper, an alternative method for evaluating the shifts in frequency and changes in intensity of the amide I, II, and III modes in solution is described. Using DFT, the shifts in frequency and intensity of the amide bands are determined in a sequence of calculations in which the positions of the solvent molecules are varied systematically. These shifts in relation to the position of the solvent are fitted directly. This process has been followed for NMA in water and acetonitrile. Using structures taken from MD simulations, band profiles for the amide I, II, and III modes are evaluated.

Computational Details

Harmonic vibrational frequencies were calculated for NMA-3H_2O and NMA-3MeCN clusters as the distances from the solute of the three solvent molecules were varied. For the NMA-3H_2O cluster, distances r_a, r_b, and r_c (Figure 2) ranged from 1.5 → 2.7 Å, 1.7 → 2.9 Å, and 1.5 → 2.7 Å in 0.2 steps, giving a total of 343 structures. For acetonitrile, r_a, r_b, and r_c (Figure 2) ranged from 2.1 → 3.6 Å, 1.6 → 3.4 Å, and 2.1 → 3.6 Å in 0.3 steps, a total of 252 structures. In these calculations, geometries were fully optimized within the constraints of these three distances. Further calculations were performed in which the harmonic frequencies of the amide modes were determined at the ground-state minimum energy structures of NMA-$n$$H_2O$ and NMA-nMeCN (n = 1−3) clusters. All calculations were performed at the EDF1/6-31+G* level with the Q-CHEM software package.[28] The effect of basis set superposition error (BSSE) can be corrected with the counterpoise correction.[29] However, in the current study no correction was introduced since it has been noted elsewhere[9] that the effect of BSSE is not very significant, particularly for the relative position of the amide bands. Further calculations were performed with the NMA-3H_2O cluster embedded in a continuum with dielectric constant of ϵ = 78.39, corresponding to water. The presence of the cavity introduces a degree of ambiguity in relation to the choice of the cavity radius. In our calculations, the spherical cavity has an origin at the center of mass of the NMA-3H_2O cluster. The

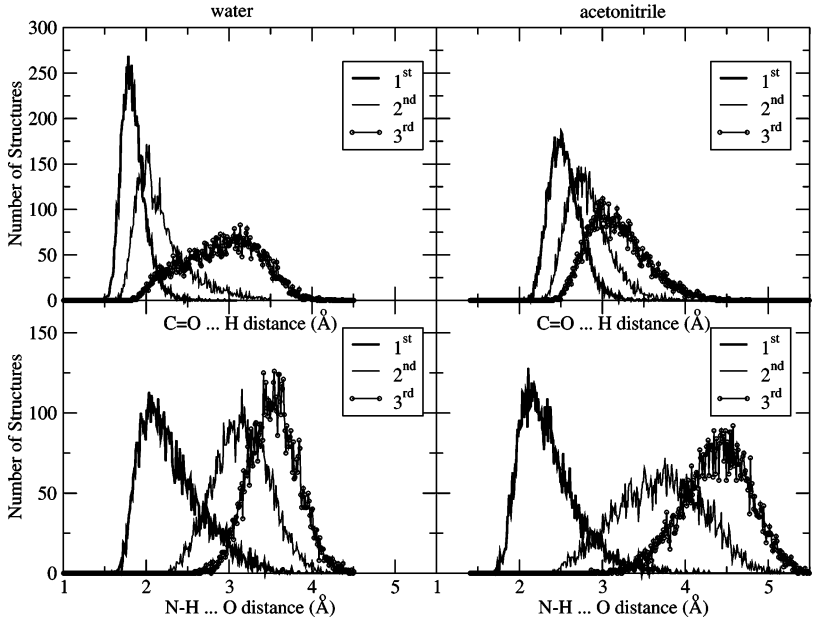

Figure 3. Distribution of NMA−solvent distances of the three closest solvent molecules to the carbonyl oxygen (top panels) and amide hydrogen (bottom panels) during the simulations.

TABLE 1: Computed Shifts in the Frequencies and Intensities of the Amide Bands in NMA-nH$_2$O (n = 1−3)

	amide I		amide II		amide III	
	frequency (cm^{-1})	intensity (km mol^{-1})	frequency (cm^{-1})	intensity (km mol^{-1})	frequency (cm^{-1})	intensity (km mol^{-1})
A	−17	+98	+18	−3	+13	+1
B	−1	0	+50	+5	+19	+35
C	−8	+81	+22	+9	+10	0
AB	−26	+92	+45	0	+27	+12
AC	−32	+107	+21	+28	+31	−22
BC	−18	+84	+50	+17	+39	+8
ABC	−45	+220	+59	+6	+54	−12
expt[a]	−106	n/a[b]	+83	n/a	+62	n/a

[a] Reference 9. [b] Not available.

hydrogen atoms of water molecules B lie predominantly furthest from the center of mass. We have chosen cavity radii of 4 Å + r_b, which allows for the distance of the water molecule B from the center of mass, the van der Waals radius of hydrogen, and an additional distance to account for "solvent packing". The shift in frequencies and changes in intensity of the amide modes are then fitted with multidimensional spline fits of the three parameters r_a, r_b, and r_c using MATHEMATICA.[30] Additional fits using less of the computed data were also performed.

MD simulations of NMA in water were performed using the CHARMM program[31] with the CHARMM22 all-hydrogen parameters.[32] These simulations had constant energy and volume. However, very similar results would be obtained using constant volume and temperature simulations. Cubic periodic boundary conditions with a box of length 18.856 Å containing one NMA molecule and 216 water molecules were also used. Intermolecular interactions were modeled by the Lennard-Jones and Coulombic potentials with water potentials on the basis of the TIP3P model.[33] For the NMA in acetonitrile simulations, a similar protocol was followed. The unit cell box had length 26.412 Å, containing NMA and 210 acetonitrile molecules. The potentials of Grabuleda et al.[34] for acetonitile were used.

All simulations consisted of an initial heating period, in which the temperature was raised to 300 K. The total heating time was 6 ps and the system was then equilibrated for a further 12 ps. During this interval, the velocities were scaled to ensure the temperature remained between 300 ± 5 K. Forty independent 200 ps simulations were performed. Two hundred structures, sampled at equal time intervals, were taken from each simulation. This gave a total of 8000 structures. For each structure, the distance of the closest solvent molecules in the A, B, and C positions were found and the frequencies and intensities of the amide I, II, and III bands were evaluated. Band profiles were then generated by distributing the calculated intensities into 0.1 cm^{-1} divisions and spectra were plotted. Band profiles without these statistical fluctuations were generated by representing each of the amide modes from all of the structures by Gaussian functions of bandwidth 10 cm^{-1}. This is smaller than the heterogeneous broadening observed and does not have a large effect on the band shape. This can be interpreted as incorporating additional broadening effects, such as lifetime broadening.[13]

Results and Discussion

Figure 3 shows the distribution of distances of the three closest solvent molecules from the NMA carbonyl oxygen and amide hydrogen during the simulations. Initially, we will focus on the simulations in water. The average carbonyl−water hydrogen bond distances are 1.85 Å, 2.18 Å, and 2.91 Å. This indicates that on average there are only two water molecules forming strong hydrogen bonds with the carbonyl group. Similarly, the average amide hydrogen−water oxygen distances are 2.31 Å, 3.15 Å, and 3.54 Å. On average, there is only one strong hydrogen bond formed with the amide hydrogen. This supports the findings of earlier work that NMA has three

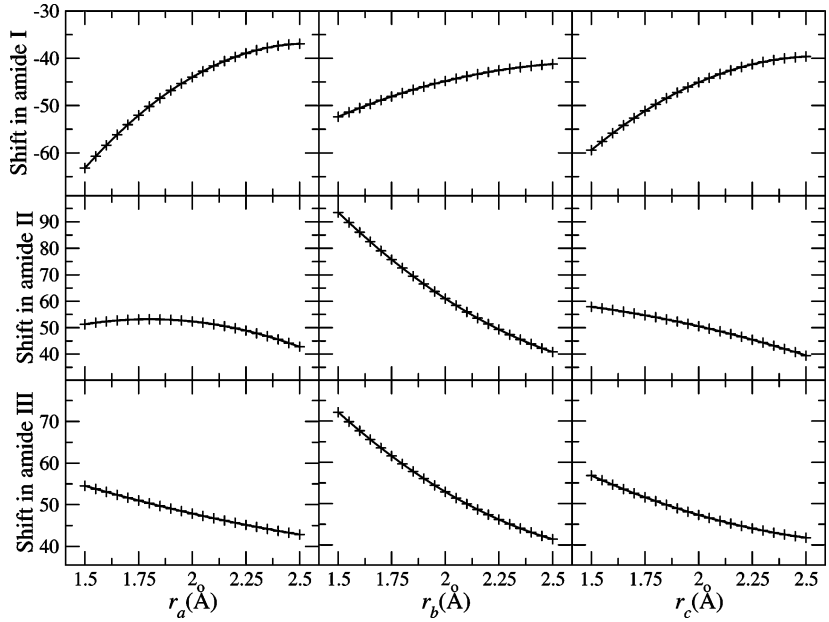

Figure 4. Variation (in cm^{-1}) of the amide frequencies with the position of the water molecules.

dominant hydrogen bond sites in solution.[35] Analysis of the NMA in acetonitrile simulations shows there is one acetonitrile molecule hydrogen bonding to the amide hydrogen. This is similar to NMA in water. In contrast, there is no distinct pattern in the distributions of carbonyl−hydrogen distances and the solvent molecules lie further from the oxygen. This reflects the lack of a strong interaction.

Computed shifts in the frequencies and intensities of the amide modes for NMA-$n$$H_2O$ ($n = 1-3$) clusters at their fully optimized structures are shown in Table 1. Introduction of one water molecule in any of the three hydrogen bonding sites leads to small frequency shifts with the correct sign. A water molecule hydrogen bonding to the amide hydrogen (site B) has little effect on the amide I mode. This is a consequence of the amide I mode being localized on the carbonyl group. The amide II and III modes contain a substantial contribution from the bending of the N−H group, and a water molecule at site B does have a large effect on these modes. Water molecules in the A and C positions have a significant effect on the amide I frequency and lead to a large increase in the amide I intensity. The inclusion of multiple solvent molecules yields an increase in the computed shifts. In the NMA-$3H_2O$ cluster, computed shifts for the amide II and III modes are approaching experiment. However, the shift in the amide I mode is considerably lower than experiment. A large increase in the amide I intensity and modest changes in the intensities of the amide II and III bands are predicted.

Earlier BPW91/6-31G* calculations predicted shifts of −62, −10, and +76 cm^{-1} for the amide I, II, and III modes, respectively.[9] In addition, the intensity of the amide I mode doubled. These shifts show some significant differences to the results presented here. In particular, at the EDF/6-31+G* level a large blue-shift in the amide II mode and a smaller increase in the intensity of the amide I mode are observed. The EDF/6-31+G* results are in closer agreement with the BPW91/6-31G* results with more diffuse polarization functions.[9] This indicates that the computed solvatochromic shifts are sensitive to the choice of theory and the presence of diffuse functions in the basis set is important.

To extend this approach to compute harmonic frequencies for a large number of clusters drawn from MD simulations presents several difficulties. First, the number of calculations required to provide adequate sampling of the solvent configurations is not practical. Second, harmonic frequencies need to be computed at an optimized structure. A structure drawn from a MD simulation would have to be reoptimized at the level of theory being used to determine the Hessian in the (harmonic) frequency analysis and structural information from the MD simulation would be lost. To overcome these problems, we have computed harmonic frequencies for a set of NMA-$3H_2O$ clusters in which the positions of the solvent are varied systematically. The geometries are fully optimized within the constraints of the three solute−solvent distances. While these structures will not correspond to the global minimum, this should not have a large effect on the computed properties of the amide modes. Analysis of the normal modes of the fully optimized NMA-$3H_2O$ cluster shows the amide I mode to be over 90% associated with the motion of the NMA atoms. For the amide II and III modes, over 99% are associated with NMA. Since within the constraints NMA is fully optimized, the deviation from the global minimum should not have a large effect. Within this approach, only the distance of the solvent from NMA is considered. Variation of the solvatochromic shifts because of variation in the orientation of the solvent is neglected.

The shifts in the frequencies and intensities vary smoothly as the position of the solvent molecules change. These data are fitted well by spline fits. For the frequency data, $R^2 = 0.96$, 0.93, and 0.97 ($n = 343$) for the amide I, II, and III modes, respectively. Correspondingly, for the intensities $R^2 = 0.86$, 0.85, and 0.95. Figure 4 illustrates the shifts in the amide bands as the position of a water molecule is varied. This figure shows how a change in the position of a water molecule in the different sites affects the amide modes. The shifts in amide frequencies will be dependent on the location of all three solvent molecules. To isolate the role of a single water molecule at a particular site, the positions of the remaining two water molecules are kept fixed in their most probable positions, 1.85 Å for A and C and 2.31 Å for B. These plots illustrate how the position of the water molecules in the three hydrogen bonding sites affects the different amide modes. The magnitude of the changes in the shifts indicate how sensitive the amide mode is to the solvent. The results reflect earlier observations based on the optimized cluster calculations.

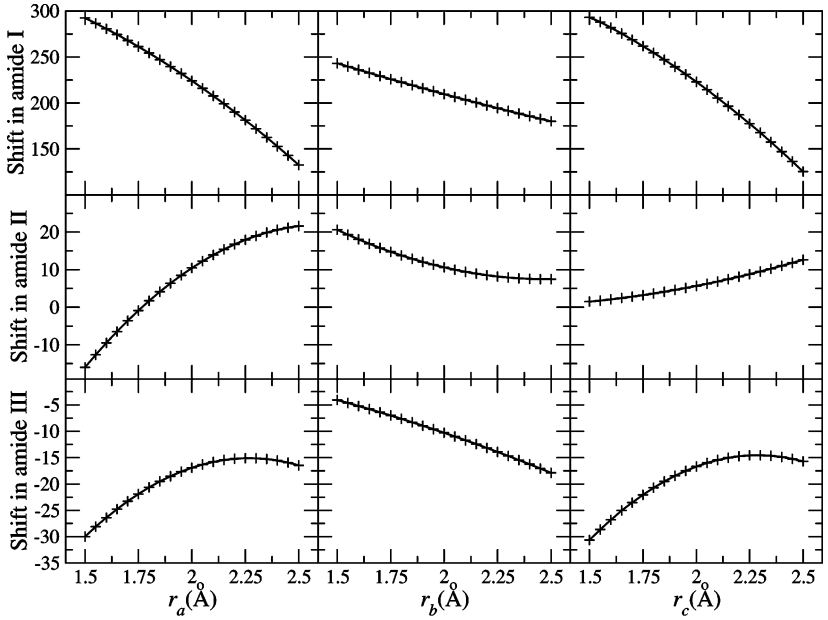

Figure 5. Variation (in km mol^{-1}) of the amide intensities with the position of the water molecules.

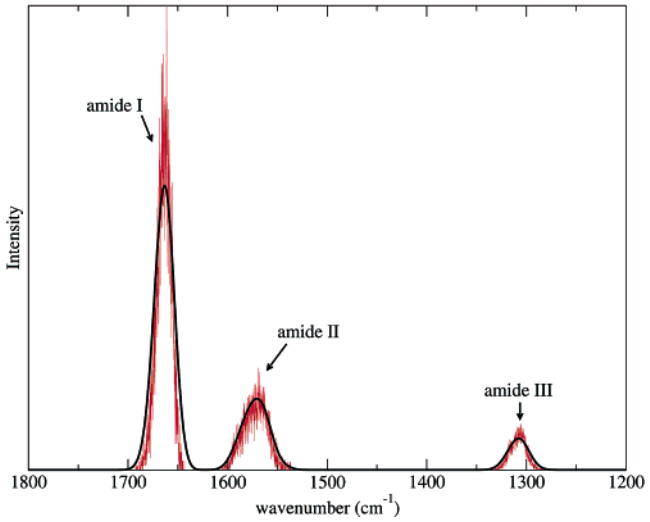

Figure 6. Computed spectra of NMA in water on the basis of NMA-3H_2O cluster calculations.

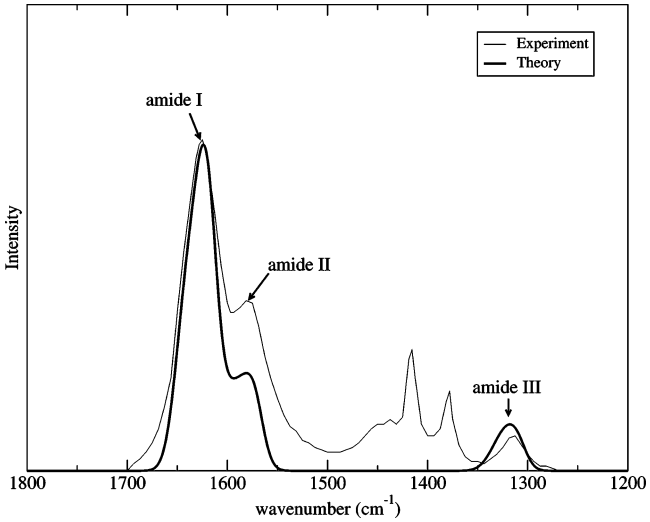

Figure 7. Computed spectrum of NMA in water on the basis of NMA-3H_2O cluster with continuum reaction field calculations (bold line) and experiment (narrow line). Experimental spectrum adapted from ref 9.

The results show a red-shift for the amide I band and blue-shifts for the amide II and III bands. The magnitude of these shifts increases as the solvent molecules become closer. As expected, the water molecule at position B has a large effect on the amide II and III modes and a much smaller effect on amide I. Solvent at the A and C positions has a large effect on amide I. However, the amide III mode is also sensitive to solvent at C. The variation of the computed intensities with respect to the position of the solvent is shown in Figure 5. The largest change is for the amide I mode. There is a large increase in intensity when solvent molecules A or C become close. More modest changes in intensity are observed for the amide II and III modes.

Figure 6 shows the computed amide band profiles in water on the basis of NMA-3H_2O cluster calculations. Eight thousand solvent configurations were sampled and the data are represented in two forms. First, the computed intensities are accumulated in 0.1 cm^{-1} divisions. For each of the amide modes, spectral bands that are Gaussian-like are obtained. This represents a direct simulation of the spectral bands. Usually, spectral bands are obtained by introducing a Gaussian profile of arbitrary width.

TABLE 2: Variation of the Computed Band Frequencies and Full Width at Half Maxima in Parentheses with the Amount of Data Used in the Fit (in cm^{-1})

grid	number of data points	amide I	amide II	amide III
full	343	1621 (38)	1582 (47)	1318 (30)
grid 2	196	1622 (39)	1580 (34)	1318 (34)
grid 3	112	1620 (41)	1581 (43)	1322 (31)
grid 4	64	1617 (35)	1581 (36)	1321 (27)

Even though 8000 configurations were sampled, the spectrum retains some roughness because of statistical fluctuations. These spectra demonstrate that solvent causes substantial broadening of the vibrational bands. Smooth band profiles are obtained when each computed amide mode is represented by a Gaussian. The smoothed spectrum follows the unbroadened representation, with a small broadening of the bands.

The computed frequencies of the amide I, II, and III modes are 1664, 1571, and 1308 cm^{-1}, respectively. The corresponding frequencies from experiment are 1625, 1582, and 1317 cm^{-1}.[9] The amide II and III frequencies are in good agreement with

TABLE 3: Computed Shifts in the Frequencies and Intensities of the Amide Bands in NMA-*n*MeCN ($n = 1-3$)

	amide I		amide II		amide III	
	frequency (cm^{-1})	intensity (km mol^{-1})	frequency (cm^{-1})	intensity (km mol^{-1})	frequency (cm^{-1})	intensity (km mol^{-1})
A	+1	+53	+10	+6	+6	+5
B	−6	+41	+20	+20	+21	+14
C	+4	+49	+4	−4	+4	+2
AB	−12	+85	+27	+21	+25	+8
AC	−4	+58	+4	+4	+4	−4
BC	−11	+92	+30	+28	+27	+11
ABC	−12	+95	+22	+22	+24	+1
expt[a]	−57	n/a[b]	+47	n/a	+30	n/a

[a] Reference 9. [b] Not available.

experiment with errors of less than 10 cm^{-1}. However, the amide I frequency is too high and the resulting amide I−amide II splitting is too large. This is consistent with the results of the NMA-3H_2O cluster calculation. As observed in previous studies,[9] a continuum dielectric in addition to explicit solvent is required to capture the shift in the amide I band. Figure 7 shows the computed spectrum based on fits derived from NMA-3H_2O clusters embedded in a continuum reaction field. This spectrum incorporates the additional broadening and is compared directly to experiment. The only adjustment to the theoretical spectrum is to scale the computed spectrum so the heights of the amide I bands match. The experimental spectrum includes additional peaks in the region 1350−1450 cm^{-1}. These correspond to vibrational modes associated with the methyl groups. We have not attempted to model these bands. Band frequencies of 1621, 1582, and 1318 cm^{-1} are obtained for the amide modes. These are in much better agreement with experiment with the large red-shift in the amide I mode reproduced. Furthermore, the computed band profiles have the correct shape. The largest deviation of the spectrum from experiment is the relative intensity of the amide II band, which is too low.

The spectra presented are based on fits to a large number of cluster calculations. The generation of these data requires considerable computational effort. Additional spectra have been generated in which less of the computed data points are used in the fitting process. The band frequencies and fwhm derived from these spectra are shown in Table 2. The full grid constitutes when data points are evaluated at 0.2 Å intervals in r_a, r_b, and r_c. In grid 2, data is included for the r_b coordinate at 0.4 Å intervals with the full data for r_a and r_c. There is little degradation in the computed frequencies; however, some deviation occurs for the fwhm of the amide II and III modes. This is most pronounced for the amide II mode. Since the water molecule at site B hydrogen bonds to the amide hydrogen, a larger effect on the amide II and III modes is expected. In the computed spectra, this leads to a loss in intensity of the amide II mode. In grid 3, the full grid is used for r_b, while r_a and r_c are included at 0.4 Å intervals. For this grid, the frequencies are reproduced and the degradation of the fwhm of the amide II and III modes is reduced. In grid 4, 0.4 Å intervals are used for r_a, r_b, and r_c. The frequencies remain good, while some degradation in the fwhm is observed. Regarding the solvent molecules as independent would require less data but would be a poorer approximation since the effects of the solvent molecules are interdependent. Overall, accurate spectra can be obtained using less data; consequently, this approach could be extended readily to other systems.

Table 3 shows the shifts in the amide modes from optimized NMA and acetonitrile clusters. The presence of acetonitrile molecules has a much smaller effect on the amide modes than water. This is particularly true for solvent in the A and C positions. This is consistent with experiment, in which smaller solvatochromic shifts are observed for acetonitrile. The strength of the interactions between NMA and acetonitrile are weaker and perturb the vibrational force field less. An acetonitrile at site B does induce a significant shift in the amide II and III modes. The predicted shifts for the NMA-3MeCN cluster are much smaller than experiment.

The theoretical and experimental spectra for NMA in acetonitrile are shown in Figure 8. The theoretical spectrum is derived from NMA-3MeCN cluster calculations. The predicted amide frequencies are 1685, 1559, and 1296 cm^{-1}, compared to the experimental values of 1674, 1546, and 1285 cm^{-1}. The agreement with experiment is not as good as for water (with the continuum parameters). However, the agreement with experiment remains quite good, with an overestimation of ~10 cm^{-1}. Furthermore, the band profiles and amide I−amide II splitting are reproduced well. It is possible that the accuracy of the computed frequencies would be improved by embedding the NMA-3MeCN cluster in a reaction field. Exploratory calculations indicate that the large spherical cavity required and relatively low dielectric constant (compared to water) resulted in the continuum dielectric having little effect on the computed IR properties. The agreement with experiment of the calculated frequencies is significantly better than would be expected from the optimum cluster calculations in which the shifts are underestimated considerably. The reason for this is that within bulk solvent the solvent molecules are closer to NMA than in the optimized geometry of the NMA-3MeCN cluster.

From these calculations, the broadening of the spectral bands because of solvent can be estimated. The fwhm of the computed

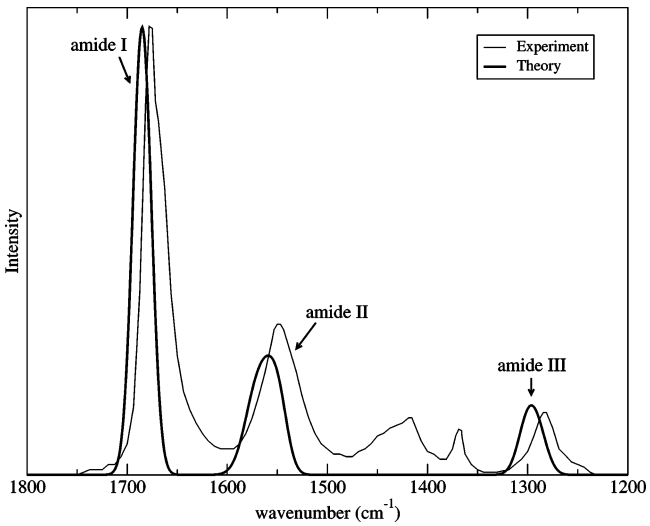

Figure 8. Computed spectrum of NMA in water on the basis of NMA-3MeCN cluster calculations (bold line) and experiment (narrow line). Experimental spectrum adapted from ref 9.

TABLE 4: Computed Amide Band Frequencies and Full Width at Half-Maxima in Parentheses (in cm^{-1})

	amide I	amide II	amide III
NMA+3H_2O	1664 (23)	1571 (31)	1308 (25)
NMA+3H_2O+continuum	1621 (38)	1582 (32)	1320 (32)
expt (water)[a]	1625 (49)	1582 (47)	1317 (30)
NMA+3MeCN	1685 (22)	1559 (39)	1296 (27)
expt (acetonitrile)[a]	1674 (27)	1546 (44)	1285 (27)

[a] Reference 9.

and experimental bands are shown in Table 4. The experimental values have been estimated from the spectra of Kubelka and Keiderling.[9] Estimation of the fwhm for the amide II band in water proved more difficult since this band overlaps with the amide I band. It is interesting to compare the extent of broadening of the amide bands in the two solvents. There is little difference in the extent of broadening of the amide II and III bands in the two solvents. However, the broadening of the amide I band in acetonitrile is approximately half. This suggests a relationship between the extent of broadening and hydrogen bonding, since acetonitrile will only hydrogen bond to the amide hydrogen.

The theoretical estimates of broadening are in quite good agreement with experiment and the feature of less broadening of the amide I band in acetonitrile is observed. Calculations of the spectrum in water show greater broadening using the parameters using fits with the continuum dielectric present. The theory tends to underestimate the broadening. This is most likely due to the present calculations only accounting for the distance between solute and solvent. Incorporating additional degrees of freedom relating to the relative orientation would lead to an increase in the spectral broadening.

Previous work[13] estimated the fwhm of the amide I mode of NMA in D_2O to be 38 cm^{-1}. This was adjusted to 27 cm^{-1} when the contribution from lifetime broadening was taken into account. A similar value was reported for NMA in H_2O. These results are in good agreement with value from experiment in D_2O of 29 cm^{-1} [7] but are smaller than the experimental value in H_2O. A similar approach based on DFT calculations predicted broadening of $\sim$50 cm^{-1} for the amide I band of NMA in D_2O.[14] The approach described in this paper gives fwhm of 38 and 22 cm^{-1} for the NMA amide I band in water and acetonitrile, respectively. The corresponding values from experiment are 49 and 27 cm^{-1}. Thus, a good level of accuracy relative to previous work is achieved.

Conclusions

In this paper, simulations of the amide bands of NMA in water and acetonitrile have been presented. The calculations show that solvent in the different hydrogen bonding sites of NMA does not affect the amide modes equally. The changes in frequency and intensity of the amide modes in relation to the position of the local solvent molecules are described on the basis of fits of model calculations. Band profiles were subsequently generated by extracting structures from MD simulations. The resultant spectra represent a theoretical simulation of the amide bands in solution. The predicted frequencies and intensities are in good agreement with experiment. Analysis of the bands suggests that hydrogen bonding plays an important role in determining the shape and location of the amide band profiles. In the future, we aim to study large polypeptides and incorporate this methodology into calculations of the amide I bands in proteins.

Acknowledgment. The author thanks Dr. Mark T. Oakley for molecular dynamics simulations of *N*-methlyacetamide in acetonitrile and the Engineering and Physical Sciences Research Council for funding, in particular for a Joint Research Equipment Initiative grant for computing equipment (GR/R62052) and the award of an Advanced Research Fellowship (GR/R77636).

References and Notes

(1) Krimm, S.; Bandekar, J. *Adv. Protein Chem.* **1986**, *38*, 181.

(2) Chen, X. G.; Schweitzer-Stenner, R.; Asher, S. A.; Mirkin, N. G.; Krimm, S. *J. Phys. Chem.* **1995**, *99*, 3074.

(3) Torii, H.; Tatsumi, T.; Tasumi, M. *J. Raman Spectrosc.* **1998**, *29*, 537.

(4) Hamm, P.; Lim, M.; Hochstrasser, R. M. *J. Phys. Chem. B* **1998**, *102*, 6123.

(5) Hamm, P.; Lim, M.; DeGrado, W. F.; Hochstrasser, R. M. *J. Chem. Phys.* **2000**, *112*, 1907.

(6) Besley, N. A.; Brienne, M.-J.; Hirst, J. D. *J. Phys. Chem. B* **2000**, *104*, 12371.

(7) Zanni, M. T.; Asplund, M. C.; Hochstrasser, R. M. *J. Chem. Phys.* **2001**, *114*, 4579.

(8) Herrebout, W. A.; Clou, K.; Desseyn, H. O. *J. Phys. Chem. A* **2001**, *105*, 4865.

(9) Kubelka, J.; Keiderling, T. A. *J. Phys. Chem. A* **2001**, *105*, 10922.

(10) Kubelka, J.; Keiderling, T. A. *J. Am. Chem. Soc.* **2001**, *123*, 12048.

(11) Rubtsov, I. V.; Wang, J.; Hochstrasser, R. M. *J. Chem. Phys.* **2003**, *118*, 7733.

(12) Ham, S.; Kim, J.-H.; Lee, H.; Cho, M. *J. Chem. Phys.* **2003**, *118*, 3491.

(13) Kwac, K.; Cho, M. *J. Chem. Phys.* **2003**, *119*, 2247.

(14) Bour, P.; Keiderling, T. A. *J. Chem. Phys.* **2003**, *119*, 11253.

(15) Choi, J.-H.; Ham, S.; Cho, M. *J. Phys. Chem. B* **2003**, *107*, 9132.

(16) Watson, T. M.; Hirst, J. D. *Phys. Chem. Chem. Phys.* **2004**, *6*, 998.

(17) Watson, T. M.; Hirst, J. D. *J. Phys. Chem. A* **2002**, *106*, 7858.

(18) Adamson, R. D.; Gill, P. M. W.; Pople, J. A. *Chem. Phys. Lett.* **1998**, *284*, 6.

(19) Krimm, S.; Abe, Y. *Proc. Natl. Acad. Sci. U.S.A.* **1972**, *69*, 2788.

(20) Torii, H.; Tasumi, M. *J. Chem. Phys.* **1992**, *96*, 3379.

(21) Tomasi, J.; Perisco, M. *Chem. Rev.* **1997**, *94*, 22027.

(22) Guo, H.; Karplus, M. *J. Phys. Chem.* **1992**, *96*, 7273.

(23) Pancoska, P.; Kubelka, J.; Keiderling, T. A. *Appl. Spectrosc.* **1999**, *53*, 655.

(24) Silvestrelli, P. L.; Bernasconi, M.; Parrinello, M. *Chem. Phys. Lett.* **1997**, *277*, 478.

(25) Gaigeot, M.-P.; Sprik, M. *J. Phys. Chem. B* **2003**, *107*, 10344.

(26) Cho, M. *J. Chem. Phys.* **2003**, *118*, 3480.

(27) Kwac, K.; Lee, H.; Cho, M. *J. Chem. Phys.* **2004**, *120*, 1477.

(28) Kong, J.; White, C. A.; Krylov, A. I.; Sherrill, C. D.; Adamson, R. D.; Furlani, T. R.; Lee, M. S.; Lee, A. M.; Gwaltney, S. R.; Adams, T. R.; Daschel, H.; Zhang, W.; Oschenfeld, C.; Gilbert, A. T. B.; Kedziora, G.; Maurice, D. R.; Nair, N.; Shao, Y.; Besley, N. A.; Maslen, P. E.; Dombroski, J. P.; Baker, J.; Byrd, E. F. C.; Voorhis, T. V.; Oumi, M.; Hirata, S.; Hsu, C. P.; Ishikawa, N.; Florian, J.; Warshel, A.; Johnson, G. B.; Gill, P. M. W.; Head-Gordon, M.; Pople, J. A. *J. Comput. Chem.* **2000**, *21*, 1532.

(29) Boys, S. F.; Bernardi, F. *Mol. Phys.* **1970**, *19*, 533.

(30) Wolfram, S. *The Mathematica Book*, 4th ed.; Wolfram Media/ Cambridge University Press: Cambridge, U.K., 1999.

(31) Brooks, B. R.; Bruccoleri, R. E.; Olafson, B. D.; States, D. J.; Swaminathan, S.; Karplus, M. *J. Comput. Chem.* **1983**, *4*, 187.

(32) MacKerell, A. D., Jr.; Bashford, D.; Bellott, M.; Dunbrack, R. L.; Evenseck, J. D.; Field, M. J.; Fischer, S.; Gao, J.; Guo, H.; Ha, S.; Joseph-McCarthy, D.; Kuchnir, L.; Kuczera, K.; Lau, F. T. K.; Mattos, C.; Michnick, S.; Ngo, T.; Nguyen, D. T.; Prodhom, B.; Reiher, W. E., III; Roux, B.; Schlenkrich, M.; Smith, J. C.; Stote, R.; Straub, J.; Watanabe, M.; Wiorkiewicz-Kuczera, J.; Yin, D.; Karplus, M. *J. Phys. Chem. B* **1998**, *102*, 3586.

(33) Jorgensen, W. L.; Chandrasekhar, J.; Madura, J. D. *J. Chem. Phys.* **1983**, *79*, 926.

(34) Grabuleda, X.; Jaime, C.; Kollman, P. A. *J. Comput. Chem.* **2000**, *21*, 901.

(35) Jorgensen, W. L.; Swenson, C. J. *J. Am. Chem. Soc.* **1985**, *107*, 1489.